Fabrication and Investigation of a Novel Composite Based on Waste Polyurethane Rigid Foam and Wood Veneer

Xuanyuan Xia,[a,b] Wenqian Cai,[a,b] Yujie Wang,[a,b] Zhongyuan Zhao [a,b,*]

The escalating demand for polyurethane rigid foams (PURF) has resulted in a substantial increase in waste polyurethane products. In view of the difficulty in recycling waste PURF, this study introduces a novel mechanical recycling process that is cost-effective and features a straightforward fabrication process for producing PUW (waste PURF combined with wood veneers), which solves the problem of low strength products obtained from mechanical recycling of PU waste. Through investigation of the PURF (ground into particles before using) particle size, core layer density, the amount of resin and thickness, the optimal fabrication process was confirmed as follows: particles with the size of 1 to 3 mm as its core layer components, 0.9 g/cm^3 as its core layer density, the addition of MDI to be 20 wt%, and 8 mm thickness of whole composite. The resulting PURF-based composite exhibited superior thermal insulation properties, mechanical strength, and sound insulation performance. The optimized PUW composite had a notably low thermal conductivity of 0.04126 W/(m·K), slightly higher than that of rock wool board (0.04 W/(m·K)). In terms of mechanical performance, the wet shear strength of the optimal PUW composite reached 0.61 MPa. Furthermore, the PUW composite exhibited relatively high sound insulation, particularly at high frequencies.

DOI: 10.15376/biores.19.3.5916-5934

Keywords: Polyurethane rigid foam; Recycling method; Composite; Thermal conductivity; Wet shear strength; Sound transmission loss

Contact information: *a: Jiangsu Co-Innovation Center of Efficient Processing and Utilization of Forest Resources, Nanjing Forestry University, Nanjing 210037, China; b: College of Furnishings and Industrial Design, Nanjing Forestry University, Nanjing 210037, China;*
** Corresponding author: Zhaozy@njfu.edu.cn (Zhongyuan Zhao)*

INTRODUCTION

Polyurethane (PU) materials have been the subject of research since the 1930s, leading to the development of a wide range of products including foams, fibers, elastomers, coatings, adhesives, and medical materials (Ionescu 2005). In recent years, the construction and furniture industries have been significant consumers of PU (Ates *et al.* 2022), with foams, particularly flexible and rigid foams, being key products in this sector (White and Durocher 2016; Beran *et al.* 2020). The versatility of foam production allows for different densities (de Mello *et al.* 2009), making it suitable for various furniture applications (Demirel and Ergun Tuna 2019), either as a thin layer combined with other materials or as the entire core (Krasny *et al.* 2001). Flexible PU foams are valued for their lightweight, durable, and comfortable properties, as well as resistance to mildew (Ates *et al.* 2022).

Polyurethane rigid foam (PURF) is widely used for its excellent mechanical properties, acoustic performance, and chemical resistance (Demharter 1998). Its low thermal conductivity has made it a preferred insulation material in refrigeration, cold storage, and transportation pipelines (Kemona and Piotrowska 2020). The demand for rigid PU foam in energy-efficient construction structures is expected to increase further in the future (Mordor Intelligence 2020). However, the widespread use of PU materials has led to the accumulation of post-consumer waste, posing challenges for disposal. Traditional methods such as landfilling and incineration are no longer sufficient due to increasing burial costs, limited space, and growing environmental awareness (Beran *et al.* 2020). As a result, there has been a focus on developing new recycling and disposal methods for polyurethane waste.

The four main methods for polyurethane recycling and disposal include mechanical recycling, chemical recycling, energy recovery, and biological degradation (Kemona and Piotrowska 2020). Each method presents unique challenges and benefits. The energy recovery method harnesses the heat energy released by incinerating polyurethane foam for recovery, yet the drawback of discharging nitrogen-containing compounds will pollute the atmosphere (Zia *et al.* 2007). Mechanical recycling involves compression molding and the use of polyurethane waste as filler. While this method offers simplicity and cost reduction, it is limited in its application range and economic value (Zhang *et al.* 2017). Chemical recovery methods involve the decomposition of polyurethane through various chemical reactions (Yang *et al.* 2012; Heiran *et al.* 2021), but the highly crosslinked nature of PURF makes this process challenging and less effective for industrial use (Yang *et al.* 2014). Moreover, the resulting product from chemical recycling poses challenges for subsequent PURF synthesis due to the presence of auxiliary components such as flame retardants (Zygmunt-Kowalska *et al.* 2023). Biological degradation, which is environmentally friendly and applicable to postconsumer waste, is still in its nascent stages (Yang *et al.* 2012). Despite promising results, polyurethane biodegradation studies are hindered by the lengthy time required to obtain results. Consequently, a significant portion of PURF materials remains inadequately recycled, leading to resource wastage and environmental pollution.

In light of the limitations of current mechanical recycling methods for waste PURF, this study proposes a novel and cost-effective mechanical recycling method. The method mainly involves the fabrication of a PUW (waste PURF combined with wood veneers) composite, which demonstrates superior thermal insulation, mechanical properties, and sound insulation. Due to use of wood veneer as raw material, this material can be better applied in home environments. Combined with the outstanding properties of this material, it provides the possibility for its application in decorative panels such as wall panels and ceilings to exert its good sound insulation and thermal insulation functions. At the same time, the good mechanical properties of PUW also make it have certain application potential in structural panels such as floorboard, partition and furniture. This innovative recycling method effectively addresses the challenges of waste PURF recycling and utilization. The PUW composite prepared in this study can be mechanically crushed again and ultimately used as a filler for other recycled products, without generating any other waste.

EXPERIMENTAL

Materials

Waste polyurethane rigid foam materials were removed from ageing public seats, manufactured by Songran Furniture Manufacturing Co., Ltd. (Foshan, China). Eucalyptus veneers, with a moisture content of approximately 9.8% and a thickness of 2.2 mm, were obtained from Yunfeng Moganshan Home Furnishings Co., Ltd. (Huzhou, China). As for the binder, 4,4'-diphenylmethane diisocyanate (MDI) was used. MDI adhesive has high bonding performance, quite good water resistance, mould inhibition, *etc*., and it will not release toxic gases after complete reaction. The MDI used in the study was purchased from Wanhua Chemical Group Co., Ltd. (Yantai, China).

Manufacture of PUW Composite

The manufacturing process of the PUW composite is illustrated in Fig. 1. Before the fabrication process, waste polyurethane rigid foam materials underwent shredding and sieving to collect particles of varying sizes. Similar to three-layer plywood, the PUW composite features a three-layer structure. It comprises eucalyptus veneer, core layer, and then another eucalyptus veneer. The waste PURF particles, sprayed with MDI, were hot-pressed at 110 °C for 5 min to form a mat, which was subsequently cut into 300 × 300 mm dimensions, constituting the core layer of PUW composite. Following this, the mat was hot-pressed with two eucalyptus veneers (300 × 300 mm), which were applied with MDI adhesive at a spread rate of 100 g/m^2 for a single veneer surface, at 130 °C for 10 min (PUW T10 and T12 were 12.5 min and 15 min, respectively). Due to the stability of PURF and the curing effect of MDI, the properties of the entire composite material hardly change for a long period of time after preparation.

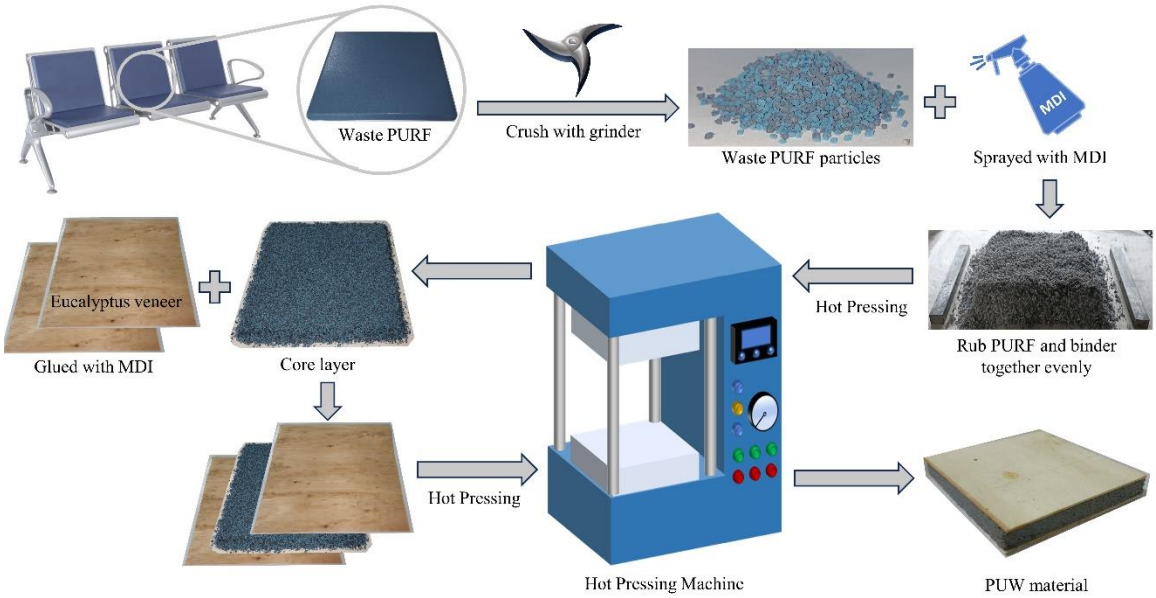

Fig. 1. The process of manufacture of PUW composite

To explore the optimal preparation process for this material, this study investigated the process from the following perspectives: particle size of rigid foam polyurethane, core density, resin content, and the overall composite thickness. The waste PURF particles were

categorized into four groups based on size: 0 to 1, 1 to 3, 3 to 5, and 5 to 7 mm. Core densities of the PUW core layer were designed to be 0.45, 0.6, 0.75 and 0.9 g/cm^3. Regarding resin content, the MDI addition amounts were 15%, 20%, 25% and 30% of the weight of PURF. In terms of thickness, 8, 10 and 12 mm were investigated. The detailed manufacturing information of all PUW composites is presented in Table 1.

Table 1. Manufacture Conditions of the PUW Composite

Samples	Particle Size (mm)	Designed Density (g/cm^3)	Resin Content (wt% of PURF)	Thickness (mm)
PUW P0-1	0-1	0.75	15	8
PUW P1-3	1-3			
PUW P3-5	3-5			
PUW P5-7	5-7			
PUW D45	1-3	0.45	15	8
PUW D60		0.6		
PUW D75		0.75		
PUW D90		0.9		
PUW R15	1-3	0.9	15	8
PUW R20			20	
PUW R25			25	
PUW R30			30	
PUW T08	1-3	0.9	20	8
PUW T10				10
PUW T12				12

Thermal Conductivity

To compare the thermal conductivity of PUW composite with plywood, a three-layer plywood with a thickness of 8 mm was prepared in this experiment. The plywood was composed of eucalyptus veneers and bonded with MDI adhesive as well, and its calculated density was approximately 0.54 g/cm^3. Subsequent to the fabrication process, samples were excised from the PUW board to dimensions of 203 × 203 mm. The thermal conductivity of PUW material was determined by heat flow meter instrument (HC-074, EKO Instrument Trading Co., Ltd, Japan). During the testing phase, the temperature of the upper and lower panel was set to 10 and 35 ℃ respectively. After the numerical value stabilized, the thermal conductivity of the specimen was recorded. Each sample was tested 5 times, and the thermal conductivity of PUW and plywood is taken as the average of 5 tests.

Shear Strength Measurement

Due to the lack of standards related to this kind of material for reference and the PUW material prepared in this study resembling three-layer plywood, comparisons were made based on China national standard *Test methods of evaluating the properties of wood-based panels and surface decorated wood-based panels* (GB/T 17657-2013) to test its shear strength as its mechanical performance. The wet shear strength measurement, an important indicator for evaluating the performance of plywood, involves immersing the specimen in water at a specified temperature, followed by shear testing to determine the strength under these conditions. The PUW materials were cut into standard tensile specimens (2.5 ×10 cm), as shown in Fig. 2. Six specimens were immersed in water (63 ± 2 °C) for 3 h and then tested by universal mechanical testing machine, at a loading rate of

10 mm/min. The procedure involved starting the universal mechanics experimental machine, applying tension to break the specimen, and recording the maximum failure load. The wet shear strength of the specimen was calculated according to Eq. 1,

$$\text{Wet shear strength (MPa)} = F / S \quad (1)$$

where F is the max failure load (N) and S is the adhesive area (mm^2).

The core layer failure frequency and adhesive layer failure frequency of each specimen were recorded. The method of calculation is shown in Fig. 3. The average value of 6 specimens were taken as the wet shear strength, core layer failure, and adhesive layer failure of PUW.

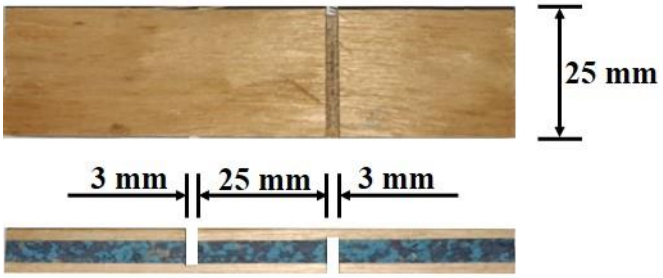

Fig. 2. The schematic diagram of specimen for wet shear strength test

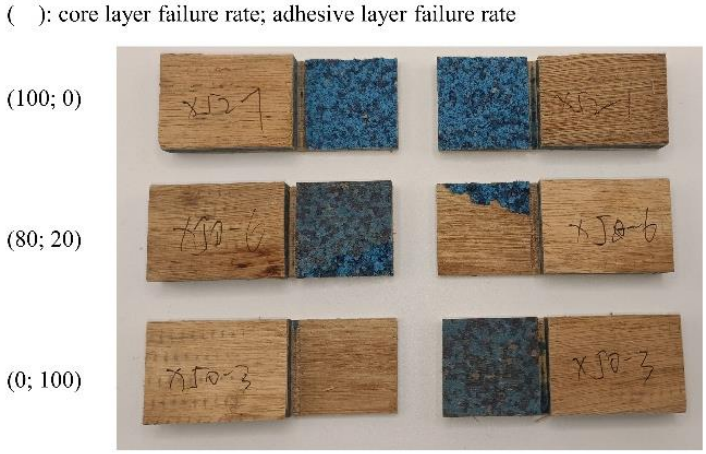

Fig. 3. The calculation method of core layer failure rate and adhesive layer failure rate

Cyclic Ageing Treatment

To test the dimensional stability, mainly described by thickness and weight change of PUW materials, cyclic ageing treatment was conducted. Specific steps were as follows: samples (cut from PUW board, 50 × 50 mm) were immersed in water (20 ℃) for 24 h; dried at 105 ℃ for 10 h; immersed in water (70 ℃) for 24 h; dried at 105 ℃ for 10 h; immersed in boiled water for 4 h; and finally dried at 105 ℃ for 10 h. After each experimental step, the thickness and weight of each specimen were recorded. Then the thickness and weight change were calculated throughout the entire processing according to Eq. 2 and Eq. 3,

$$\text{Thickness change (\%)} = [(T_1 - T_0) / T_0] \times 100\% \quad (2)$$

$$\text{Weight change (\%)} = [(W_1 - W_0) / W_0] \times 100\% \quad (3)$$

where T_1 is the thickness of PUW composite after processing, T_0 is its initial thickness, W_1 is the weight of PUW composite after processing, and W_0 is its initial weight.

Acoustical Properties

To test the sound insulation characteristics of PUW composite materials, their sound insulation was tested according to the international standard ISO 12999-2:2020 (2020). The sound insulation of all samples was measured using the four-microphone impedance tube method. The impedance tube models were SW422 and SW447 (BSWA Technology, Beijing, China), with an inner diameter of 100 mm for SW422 and 30 mm for SW447. Firstly, the PUW composite material samples were prepared into circular specimens with diameters of 100 mm and 30 mm. Then, two different sizes of specimens were placed in SW422 and SW447 impedance tubes, with a frequency range of 50 to 10 kHz. The noise and vibration testing and analysis system VA-Lab (developed by BSWA Technology, Beijing, China) was used for testing, and the sound insulation within this frequency range was finally measured.

Attenuated Total Reflectance Fourier Transform Infrared Spectroscopy (ATR-FTIR)

To investigate molecular transformation between PURF and MDI, as well as eucalyptus and MDI, an ATR FT-IR spectrophotometer (Nicolet iS10, Thermo, Waltham, MA, USA) was used. Five groups of samples were prepared. Each preparation method was as follows: (a) The PURF particles and MDI were mixed in a 5:1 ratio. (b) The mixture of PURF particles and MDI was prepared in a 5:1 ratio, followed by hot pressing at 130 °C for 10 min. (c) Eucalyptus wood powder was added. (d) The mixture of eucalyptus wood powder and MDI was prepared in a 5:1 ratio. (e) Hot pressing was done at 130 °C for 10 min. Prior to the spectroscopic analysis, all samples were ground into particles. The tests were then conducted with an average of 32 scans at a resolution of 4 cm^{-1} on the ATR FT-IR spectrophotometer.

Morphological Analysis

The microstructural morphology of the PUW composite was analyzed using a Scanning Electron Microscope (TM-1000, HITACHI, Tokyo, Japan) to investigate the effect of particle size of PURF particles on the thermal conductivity and bonding strength of PUW materials. All specimens to be observed were cut into approximately 2 mm thick samples and underwent surface gold spraying treatment in a vacuum environment. The cross-section of PUW composite material was observed with a magnification of 50 to 100 times.

RESULTS and DISCUSSION

Effects of Particle Size on Composite Properties

The impacts of PURF particle size on the properties of PUW composites are shown in Fig. 4. Part 4(a) shows the effect of particle size on the thermal conductivity of PUW. Notably, the core layer of PUW composites exhibited a positive correlation between particle size and thermal conductivity, with smaller PURF particles tending to enhance the thermal insulation performance of PUW composite. This may be due to the smaller particle size of the core layer containing more closed pores, resulting in lower thermal conductivity

(Zhang *et al.* 2017). When the particle size ranged from 0 to 1 mm, the thermal conductivity of PUW was 0.03768 W/(m·K), slightly lower than the 0.04 W/(m·K) of conventional insulation material rock wool board, indicating that PUW composite has good insulation properties. Upon transitioning to particle sizes of 1 to 3 mm, a notable 81% escalation in thermal conductivity is observed, culminating in a value of 0.0685 W/(m·K). Despite this increase, the thermal conductivity remained significantly lower than that of plywood with analogous wood thickness, which registers at 0.23 W/(m·K). This underscores the efficacy of using PURF as the core layer of PUW composite to bolster the thermal insulation capabilities.

Figure 4(b) delves into the impact of core particle size on the wet shear strength of PUW. Experimental findings unveiled a direct rise in wet shear strength with escalating PURF particle size. Notably, for particle sizes ranging from 0 to 1 mm, the wet shear strength of PUW was only 0.25 MPa, with the core layer exhibiting a 100% failure frequency. This diminution in strength can be attributed to the heightened specific surface area of smaller particles, leading to inadequate bonding strength at the interfaces. A transition to particle sizes of 1 to 3 mm led to a remarkable increase in wet shear strength to 0.54 MPa, marking a substantial 116% enhancement *vis-a-vis* the 0 to 1 mm particle size. According to the results in the graph, overall, the larger the particle size, the higher the wet shear strength.

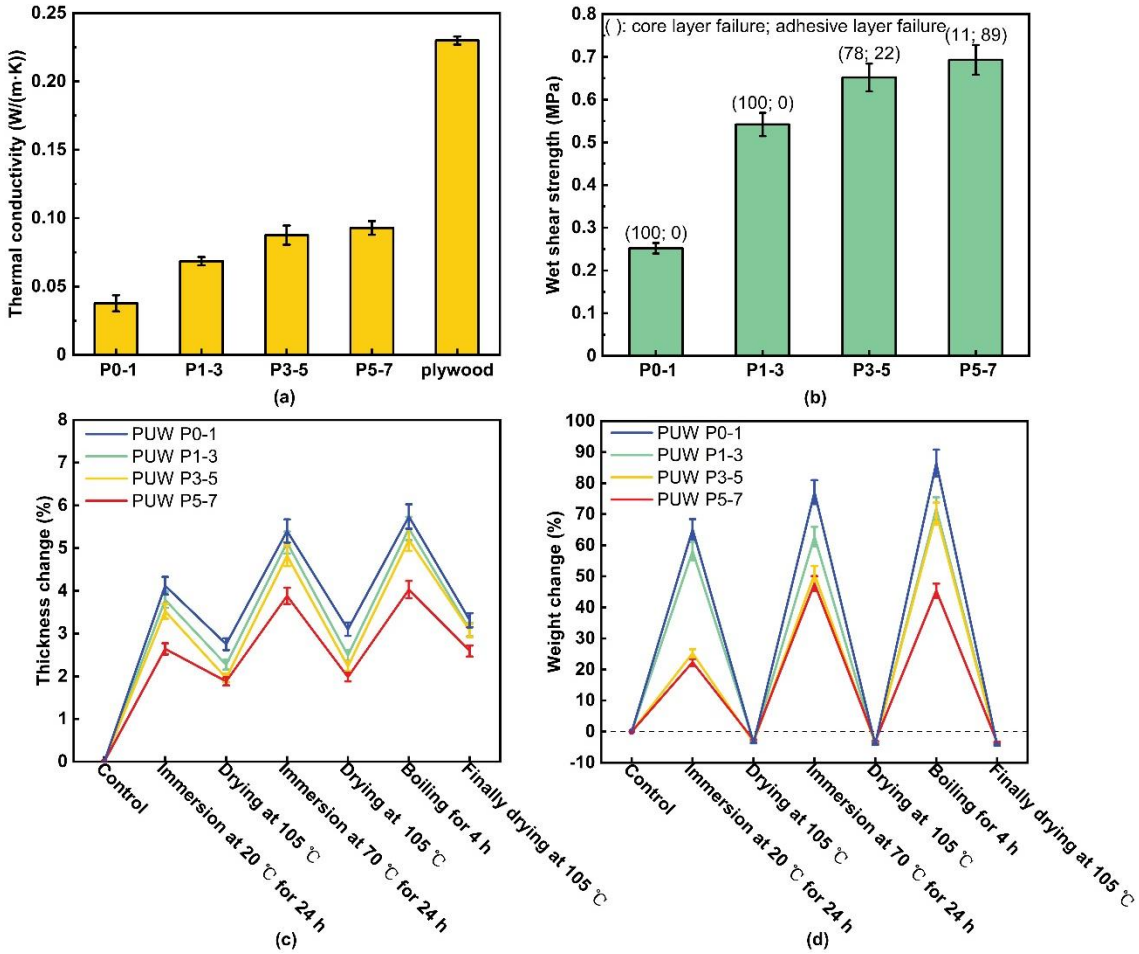

Fig. 4. Effects of the particle size on the thermal conductivity (a) and wet shear strength (b) of PUW materials. Thickness change (c) and weight change (d) during cyclic aging treatment of the PUW materials composed of different particle sizes

The thickness change percentage of each group of PUW composite in the cyclic ageing treatment is revealed in Fig. 4(c). The results show that in various accelerated degradation experiments, the thickness change of PUW with larger particle size was lower. In the first step of experiments (after soaking in cold water for 24 hours), the thickness expansion of all groups of PUW was between 2.64% and 4.12%. Comparative analysis against the 12% benchmark delineated by the JIS particleboard test standard (JIS A 5908:2015), PUW revealed notable low wet swelling. Significantly, the PUW P0-1mm consistently manifested higher thickness change relative to their counterparts. This disparity can be attributed to the inverse relationship between particle size and specific surface area within the core layer. Therefore, when the adhesive amount was the same, the bonding effect between smaller particles in the core layer was poor, resulting in a higher thickness change in cyclic ageing treatment.

Figure 4(d) shows the weight change of each group of PUW composite materials in the cyclic ageing treatment. Analogous to the trends observed in the thickness change, PUW specimens featuring larger particle sizes evinced lower weight changes. The reason may still be related to smaller particles' large specific surface and relatively poor bonding ability.

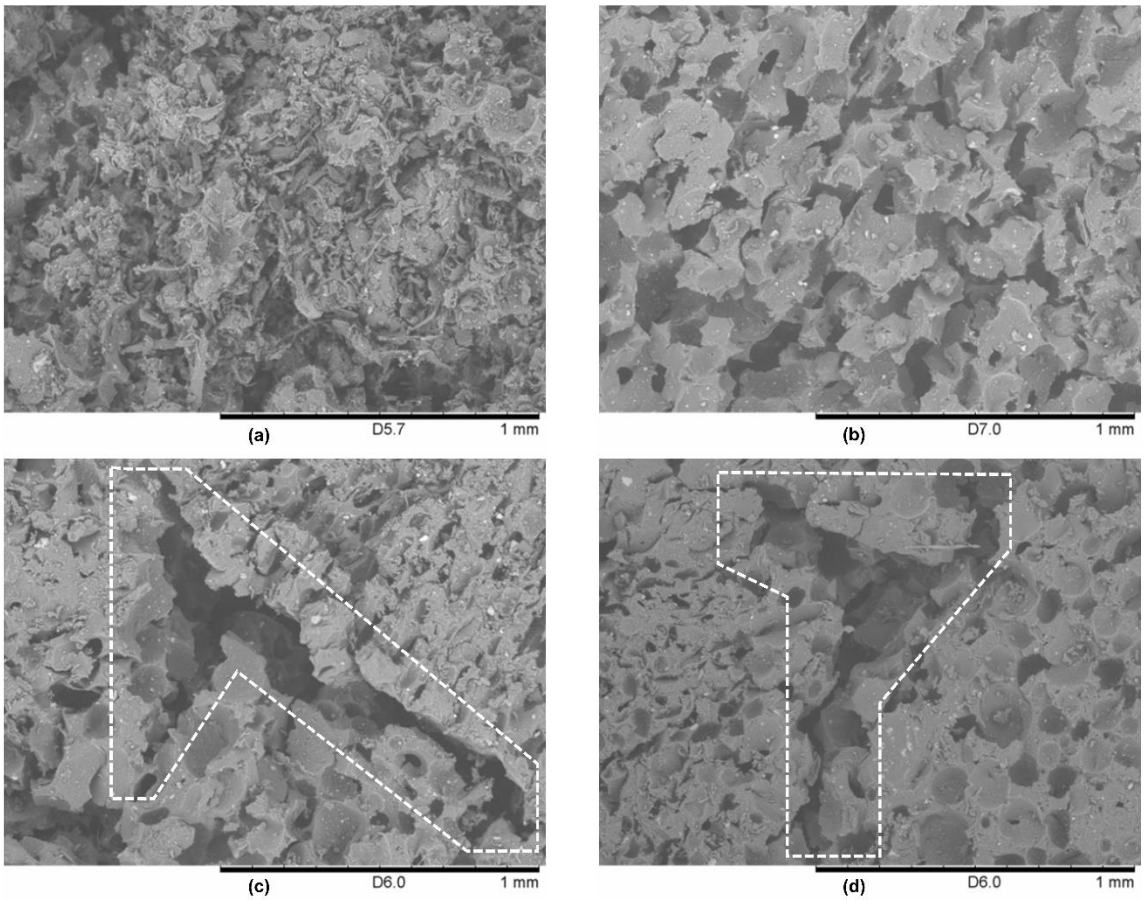

Fig. 5. SEM observation results of the PUW materials composed of different particle sizes (a) PUW P0-1, (b) PUW P1-3, (c) PUW P3-5, (d) PUW P5-7

To clarify the influence of particle size in the core layer on the various properties of PUW composite materials, SEM was carried out to scan the core layers of PUW prepared with different particle sizes (Fig. 5), thereby unraveling the microstructural of the composite. The cellular-like structure and almost all closed pores in polyurethane material contribute to a notable thermal conductivity range of 0.022 to 0.035 W/(m·K) (Demharter, 1998). Figure 5 (a) shows the internal structure of PUW P0-1. There were many pores inside that were sealed by curing MDI, finally cellular structure similar to PU was formed, thus resulting in low thermal conductivity. However, it is precisely because more MDI was used to seal pores that there was less adhesive used for inter-particle bonding. This explains why PUW P0-1 resulted in a relatively low thermal conductivity of 0.03768 W/(m·K) but also low wet shear strength. Conversely, Fig. 5(c) and 5(d) spotlight particles spanning 3-5 mm and 5 to 7 mm. They retained more closed pore structures than smaller particles, so the most parts of MDI were used for bonding between particles, leading to higher wet shear strength and lower core layer failure. But from the areas marked in the figure, it can be seen that the gaps between particles were too large to be sealed by MDI, thus leading to air circulation in this open space, resulting in higher thermal conductivity and reduced insulation performance.

In summation, while the PUW P0-1 brought out the lowest thermal conductivity, it concurrently exhibited the lowest wet shear strength and worst moisture absorption stability in cyclic ageing treatment. In stark contrast, the PUW P1-3 had a lower thermal conductivity but higher wet shear strength and better moisture absorption stability. Consequently, PURF characterized by a particle size falling within 1 to 3 mm emerged as the preferred raw material for subsequent process of PUW fabrication.

Effects of Density on Composite Properties

To investigate the effects of core density on PUW properties, several densities (0.45,0.6,0.75 and 0.9 g/cm^3) of the PU core layer were prepared before fabricating the composite. Figure 6 shows the effect of core layer density on the various properties of PUW composite materials. Figure 6(a) proclaims a negative relationship between thermal conductivity and density, indicating that a higher core density will result in better thermal insulation performance of PUW composite. When the core density was 0.45 g/cm³ (PUW D45), the thermal conductivity of the composite stood at 0.1559 W/(m·K). In stark contrast, at a core density of 0.9 g/cm³ (PUW D90), the thermal conductivity was reduced to a mere 0.05331 W/(m·K), marking a substantial 65.8% reduction *vis-a-vis* PUW D45. This salient trend can be ascribed to the smaller gap between PURF particles. Due to the formation of smaller pores between particles in the higher density core layer, the higher the density of the core layer, and the lower the thermal conductivity (Zhang et al., 2017).

Figure 6(b) reveals a positive correlation between wet shear strength and density, wherein the wet shear strength increased with increasing density. The wet shear strength of PUW D45 was 0.12 MPa, and PUW D90 was up to 0.61 MPa, marking a 408.3% surge. This phenomenon is perhaps due to the lower density, and hence the lower the internal bonding strength of core layer. The changes of core layer failure, which were not 100% until the density reached 0.9 g/cm³, also support this conjecture.

Figure 6(c) shows the thickness change of each group of PUW composites under cyclic ageing treatment, revealing the negative correlation between thickness change and density. This trend may be attributed to the fact that as the core density increased, PUW composite had an elasticity more similar to PU. For PUW D90, the maximum thickness change merely registered at 6.44%, well below the upper limit of 12% in JIS particleboard

testing standard (JIS A 5908:2015). PUW composite material exhibits low wet swelling, reflecting its excellent moisture absorption stability.

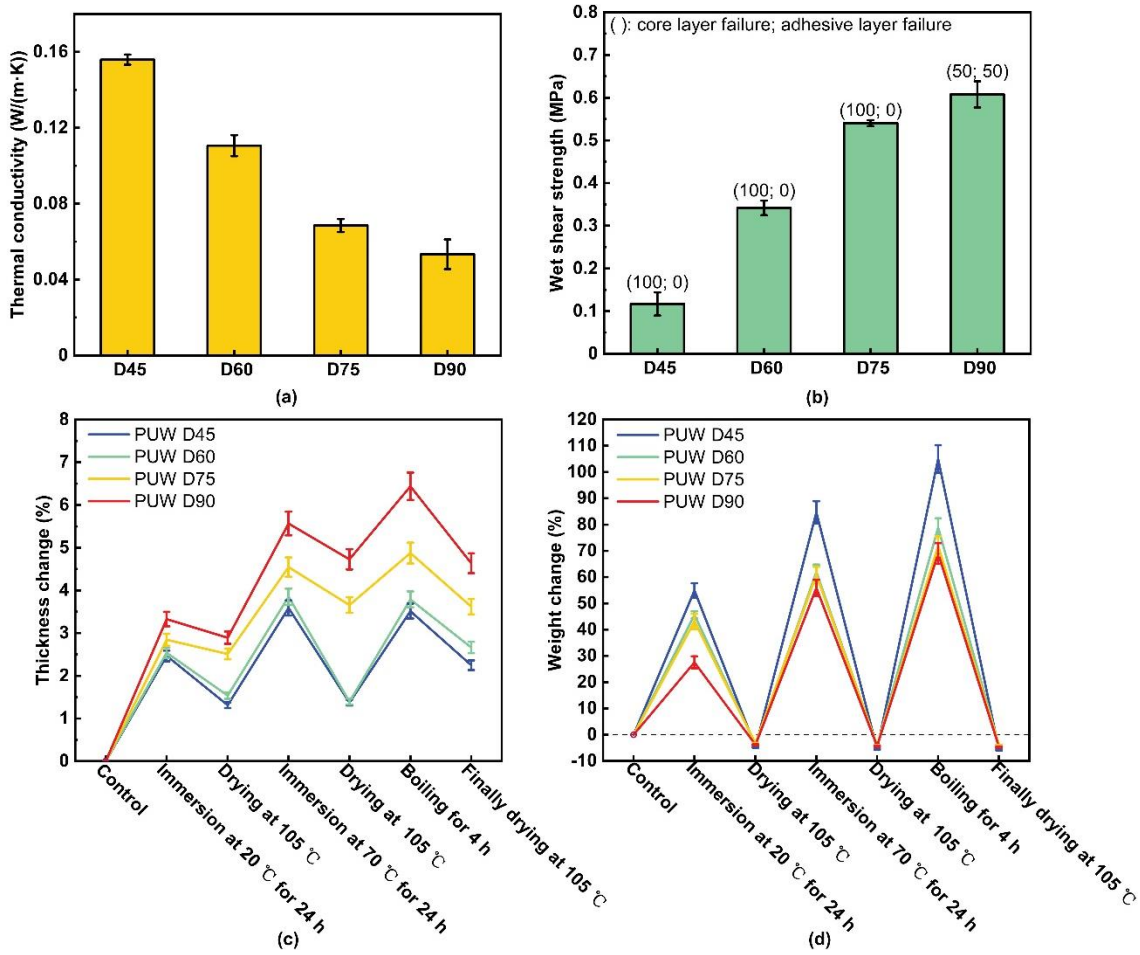

Fig. 6. Effects of the density on the thermal conductivity (a) and wet shear strength (b) of PUW materials. Thickness change (c) and weight change (d) during cyclic aging treatment of the PUW materials of different density.

In contrast to the thickness change during cyclic ageing treatment, the weight change of PUW composite with higher core density was lower, which is shown in Fig. 6(d). The reason for this phenomenon might be that the core layer with lower density had larger gaps, so it had more space to hold water, so the weight change after immersion was higher. In summary, PUW D90 exhibited relatively low levels of thickness and weight change during accelerated aging treatment, while having the lowest thermal conductivity and highest wet shear strength in this group. Therefore, 0.9 g/cm^3 was selected as the optimal density for the core layer of PUW composite materials.

Effects of Resin Content on Composite Properties

The effects of resin content on properties of PUW materials are shown in Fig. 7. Part 7(a) reveals that as the additional amount of MDI increased, the thermal conductivity showed a trend of first decreasing and then increasing. Notably, when the additional amount of MDI was 20 wt% of PURF, there was a significantly lower thermal conductivity of 0.04126 W/(m·K). The reason for this result may be that when the resin content was 15

wt%, the enclosed pores of PURF particles absorbed some MDI for filling, causing insufficient MDI for bonding the gaps between particles. Consequently, air was able to circulate in the gaps between particles, leading to an increase in thermal conductivity. As the MDI addition amount ascended to 25 wt% and 30 wt%, excess MDI filled the gaps and pores between particles after curing. This makes for the decrease in porosity, thus leading to a decrease in insulation performance.

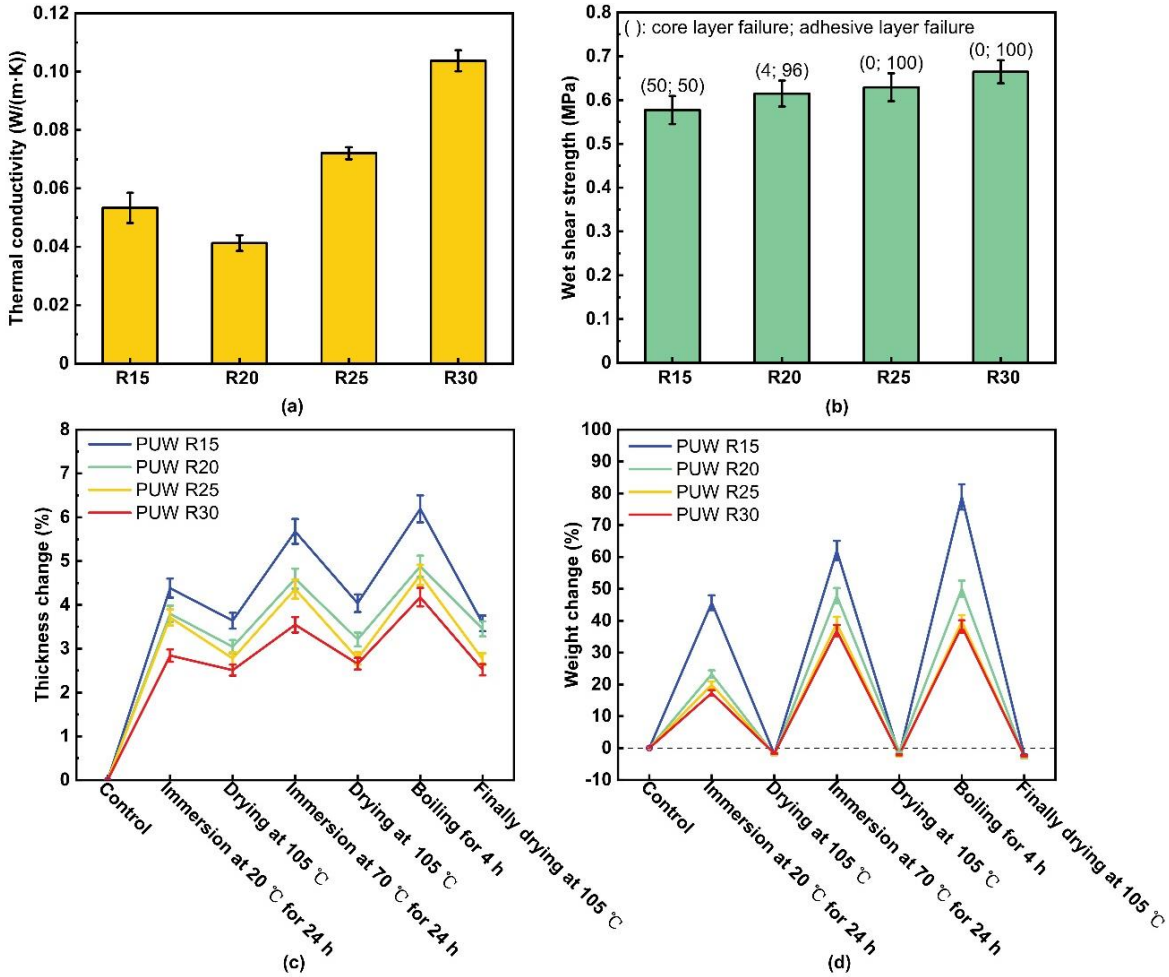

Fig. 7. Effects of the resin content on the thermal conductivity (a) and wet shear strength (b) of PUW materials. Thickness change (c) and weight change (d) during cyclic aging treatment of the PUW materials with different resin content

The results in Fig. 7(b) show that as the amount of MDI gradually increased, the increase in wet shear strength of PUW composite material was relatively small. The graph revealed a modest rise in wet shear strength as the MDI addition amount ascended from 15 wt% to 30 wt%, with an increase from 0.57 to 0.66 MPa, marking a 15.8% growth. When the MDI addition amount changed from 20 to 25 wt%, the wet shear strength increased from 0.61 to 0.63 MPa, with an increase of only 3.3%. This indicates that increasing the amount of MDI applied had limited effect on improving the wet shear strength of PUW composite materials. Noteworthy is the precipitous decline in the core layer failure percentage of PUW composite, dwindling from 50% at 15 wt% to a mere 4.2% at 20 wt%, a 45.8% reduction. This finding underscores the pivotal role of MDI application rates in internal bonding strength.

Figure 7 (c) shows the thickness change of each group of PUW composite in the cyclic ageing treatment. The results show that with the increase of MDI addition amount, the thickness change of PUW composite materials decreases. This is because the bonding effect of MDI became more significant with the increase of addition amount, and the rebound of the core layer PURF decreased due to the influence of the bonding effect, thereby reducing the overall thickness change of PUW.

The weight change of each group of PUW composite in the cyclic ageing treatment is shown in Fig. 7(d). The results show a similar trend as Fig. 7(c); that is, with the increase of MDI application amount, the weight change of PUW composite materials gradually decreased. The reason for this phenomenon may be that with the increase of MDI amount, the curing MDI fills the gap between PURF particles in the core layer, making the space for water to be accommodated smaller, resulting in a decrease in the overall quality change of PUW composite. It is worth noting that the increasing MDI amount gradually reduced its impact on the weight change. Therefore, the optimal addition amount of MDI was selected to be 20 wt%, which had the lowest thermal conductivity but relatively high wet shear strength and better wet swelling stability.

Effects of Thickness on Composite Properties

The effects of the entire thickness of PUW composite on their various properties are shown in Fig. 8. Figure 8(a) reveals a nuanced diminution in thermal conductivity as thickness escalated, with values of 0.04126, 0.03959, and 0.03734 W/(m·K) recorded for PUW T08, T10, and T12, respectively. By contrast, PUW T08, PUW T10, and T12 decreased by 4.22% and 10.5%, respectively. This indicates that the increase in thickness resulted in limited improvement of the thermal insulation performance of PUW composite.

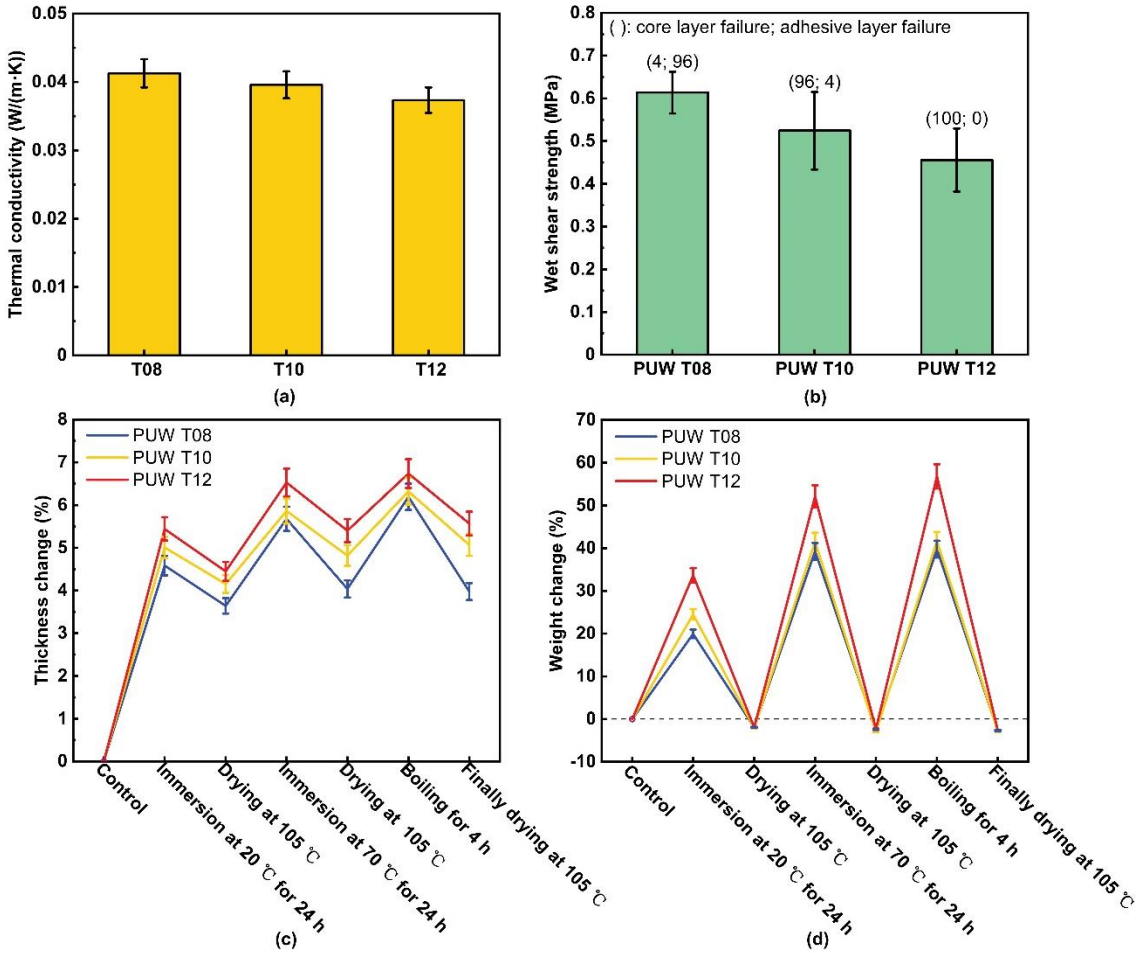

Fig. 8. Effects of the thickness on the thermal conductivity (a) wet shear strength (b) of PUW materials. Thickness change (c) and weight change (d) during cyclic aging treatment of the PUW materials of different thickness.

Figure 8(b) shows that as the overall thickness of the PUW composite material increased, its wet shear strength significantly decreased. The wet shear strength of PUW T08, T10, and T12 were 0.61, 0.52, and 0.46 MPa, respectively. Compared with PUW T08, the wet shear strength of T10 and T12 decreased by 14.8% and 24.6% respectively. The wet shear strength specimens in Fig. 9 also illuminated this trend: as the PUW composite became thicker, the core layer failure became more severe, and the core layer failure frequency increased from 4.2% to 100%. This means that the decrease in wet shear strength was related to the poor bonding performance.

Figure 8(c) focuses on the thickness change of each group of PUW composite under cyclic ageing treatment, unveiling a correlative increase in thickness change with rising overall thickness. This is because as the thickness increases, the rebound performance of the core layer PURF becomes more prominent. Notably, even PUW T12 exhibited a maximum thickness change of 6.74%. It had not yet reached the prescribed upper limit of 12% in the JIS A 5908:2015 particleboard test standard, underscoring its quite good wet swelling stability.

Similar to the thickness change, as the overall thickness of the PUW composite material increased, the weight change of the PUW composite material gradually increased (Fig. 8d). This might still be due to the rebound effect of PURF, creating additional space

for water absorption and culminating in an overall escalation in material weight change. Although the thermal conductivity of PUW T08 was the highest, as the thickness increased, the decrease in thermal conductivity of PUW T10 and T12 was relatively low, while the wet shear strength decreased significantly. In addition, the magnitudes of thickness and weight change of PUW T10 and T12 were also greater during cyclic ageing treatment. Therefore, 8 mm was chosen as the optimal thickness for the entire PUW material.

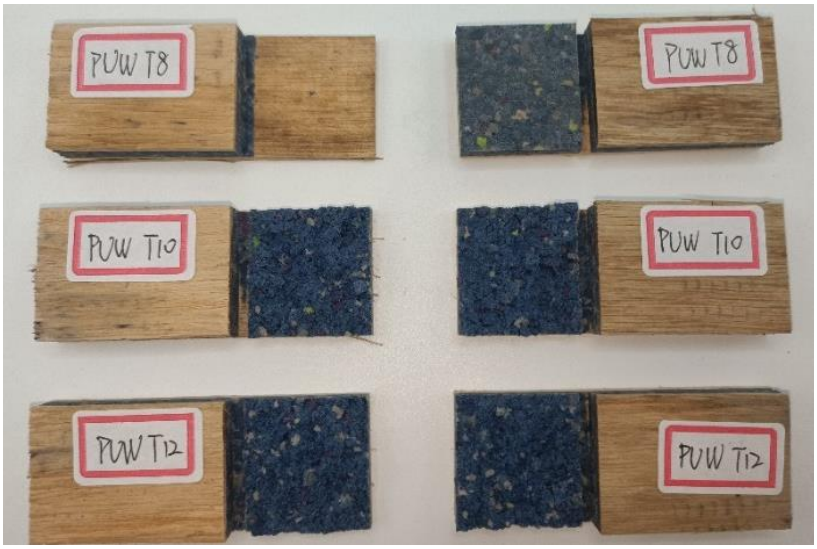

Fig. 9. The wet shear strength specimens of PUW T8, T10, T12

Sound Isolation Properties

Figure 10 shows the sound insulation of the PUW composite, with the highest sound transmission loss, at 1000 to 6500 Hz. It can be seen that the sound transmission loss of all PUW materials showed a decreasing trend at 1000 to 1500 Hz and an increasing trend after 1500 Hz.

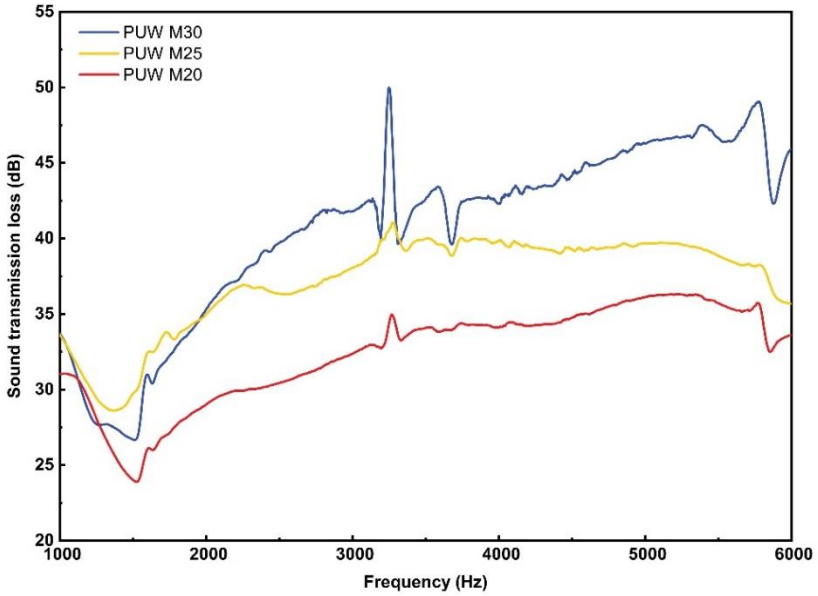

Fig. 10. Sound transmission loss of PUW M20, M25, and M30

It is worth noting that the maximum sound transmission loss of all PUW materials in this group occurred between 3000 and 3500 Hz. When the MDI adhesive application amount reached 30 wt%, its sound transmission loss reached 50.0 dB, which is higher than the maximum of lightweight partition wall materials currently used in residential buildings on the market, such as paper faced gypsum board, fiber-reinforced water mud board, ceramic aggregate concrete, *etc*. (Chen *et al.* 2011). This result indicates that the PUW has fairly good sound insulation within this frequency range.

Furthermore, as the additional amount of MDI increased, the maximum sound transmission loss perked up. A reasonable explanation is that after hot pressing and curing, the gaps and pores between the particles of the PUW core layer became filled by more MDI, resulting in improved sound insulation performance. Compared to traditional single-layer and double-layer boards, multi-layer boards have better sound insulation performance at middle or high frequency, but poor soundproofing performance at low frequency range (Zhao *et al.* 2010). PUW composite materials are similar to three-layer boards, with low sound transmission loss at low frequency conditions and relatively high sound insulation at high frequency conditions, which is consistent with the conclusions of relevant research.

ATR FT-IR Analysis

To unravel the molecular changes between MDI and PURF, alongside MDI and eucalyptus veneer, five groups of samples were prepared and then scanned by ATR-FTIR spectroscopy. The infrared spectroscopy test results are shown in Figs. 11 and 12.

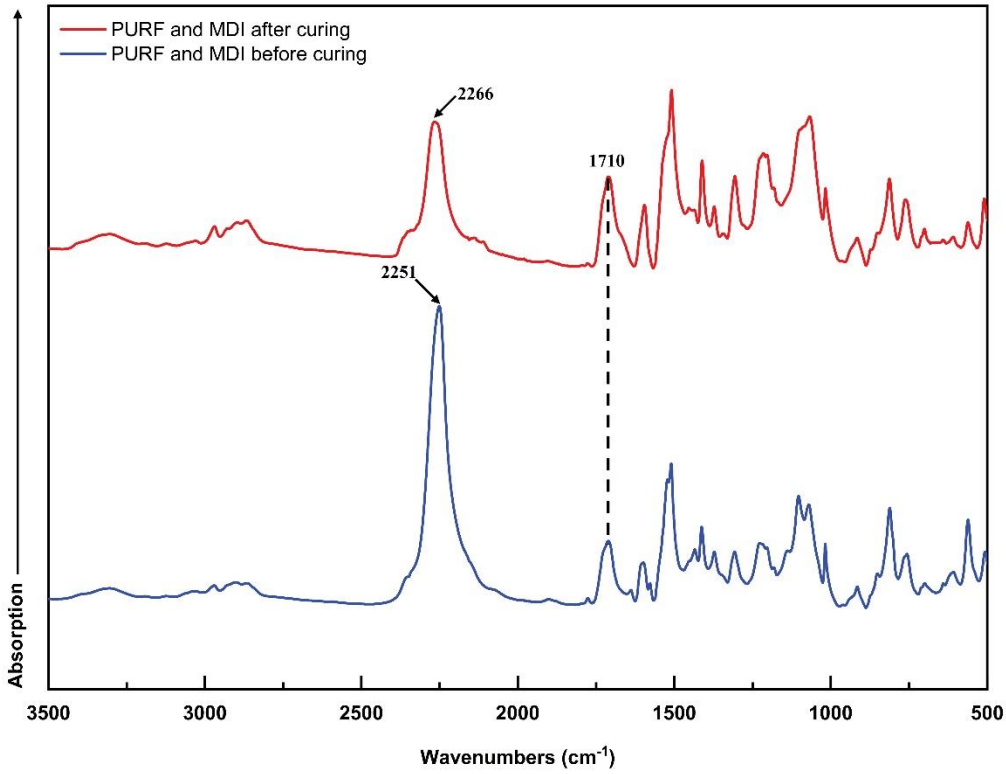

Fig. 11. ATR FT-IR infrared spectra of mixture of PURF and MDI before and after hot pressing

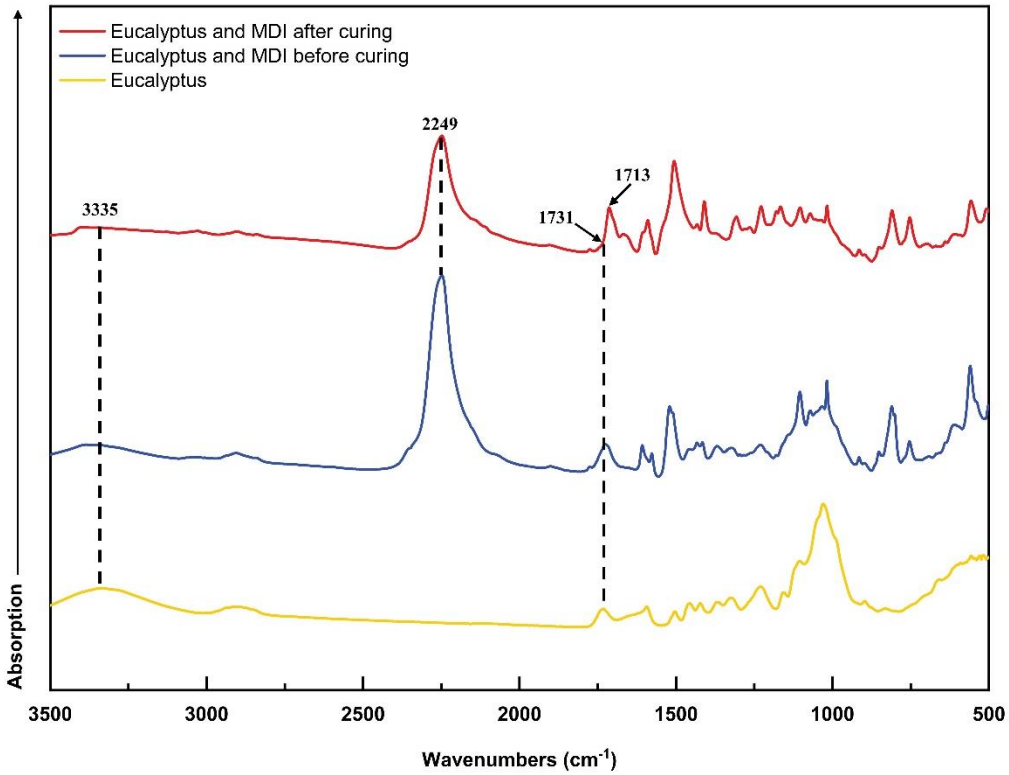

Fig. 12. ATR FT-IR spectra of eucalyptus, MDI and their mixture before and after hot pressing

Figure 11 shows the infrared spectra of PURF and its mixture with MDI before and after hot pressing. By comparison, it can be observed that one absorbance peak was weakened and one absorbance peak was enhanced. The absorbance peaks at 2266 and 2251 cm^{-1} correspond to the -N=C=O stretching vibration of the isocyanate group in MDI adhesive (Du *et al.* 2008), which weakened after hot pressing, indicating that the isocyanate was consumed in the course of hot pressing. The absorbance peak at 1710 cm^{-1} belongs to the C=O stretching vibration of the urethane groups (Li *et al.* 2008), which was enhanced after hot pressing, indicating the formation of new urethane bonds in the mixture of MDI and PURF after hot pressing.

The ATR FT-IR spectra of eucalyptus wood, MDI, and their mixture before and after hot pressing are shown in Fig. 12. In the graph, two absorbance peaks disappeared, one new absorbance peak appeared, and one weakened peak could be observed. The peak at 3335 cm^{-1} corresponds to the stretching vibration of hydrogen bonded OH group in the wood component (Gonultas and Candan 2018), the absorbance peak at 1731 cm^{-1} belongs to the stretching vibration of the carbonyl C=O of the acetoxy group in xylan (Ates *et al.* 2009), and the weakened absorbance peak at 2249 cm^{-1} corresponds to the stretching vibration of the isocyanate group N=C=O in MDI. The newly added peak at 1713 cm^{-1} corresponds to the C=O stretching vibration of the amino ester group, indicating that the hydroxyl groups in eucalyptus wood form urethane bonds with MDI after hot pressing. The possible reaction mechanism between PURF and MDI, as well as eucalyptus and MDI is shown in Fig. 13. In the core layer of PUW, urethane bonds formed between PURF and MDI. When it comes to the interface between eucalyptus wood and PURF, the OH group of eucalyptus wood and N=C=O of MDI formed new urethane bonds as well.

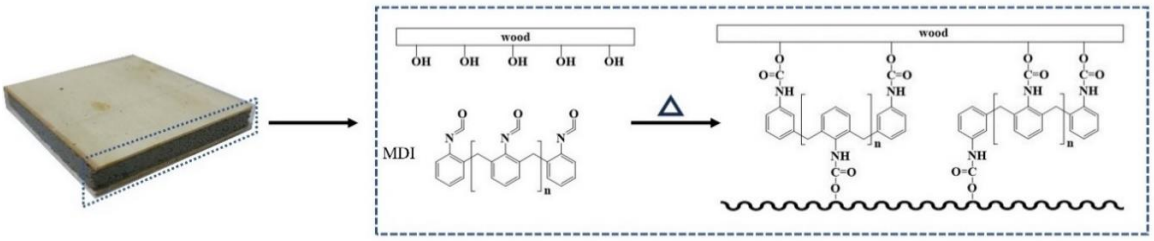

Fig. 13. Possible reactions among eucalyptus wood and MDI

This investigation presented an innovative approach to mechanically recycle PURF, offering a cost-effective and straightforward method for fabricating PURF-based materials. This study, to some extent, solves the problem of low strength and low grade products obtained from mechanical recycling of PU waste. Future endeavors will focus on enhancing the bonding performance, particularly focusing on augmenting the internal bond strength of the core layer and fortifying the dimensional stability of the overall PUW material. These concerted efforts aim to bolster the recycling value of PURF, charting a course towards sustainable material utilization and resource conservation.

CONCLUSIONS

1. Through a comprehensive analysis encompassing thermal conductivity assessments, wet shear strength evaluations, and cyclic ageing treatments, the best fabrication method for polyurethane rigid foam (PURF) utilized 1- to 3-mm crushed PURF particles as the core layer components, with a core layer density of 0.9 g/cm³ and a 20 wt.% addition of 4,4'-diphenylmethane diisocyanate (MDI), which was then combined with eucalyptus wood veneers in an 8 mm composite thickness.
2. The resultant PUW composite exhibited a notably low thermal conductivity of 0.04126 W/(m·K) and showed relatively high mechanical properties, boasting a wet shear strength of up to 0.61 MPa. Furthermore, the investigation revealed promising sound insulation capabilities within the high frequency range. Attenuated total reflection Fourier transform infrared (ATR FT-IR) analyses corroborated the formation of novel urethane bonds between PURF and MDI, as well as at the interface of eucalyptus wood and MDI, shedding light on the excellent bonding performance of PUW.

ACKNOWLEDGEMENTS

The authors are grateful for the testing support by Advanced Analysis and Testing Center of Nanjing Forestry University.

REFERENCES CITED

Ates, M., Karadag, S., Eker, A. A., and Eker, B. (2022). "Polyurethane foam materials and their industrial applications," *Polym. Int.* 71(10), 1157-1163. DOI: 10.1002/pi.6441

Ates, S., Akyildiz, M. H., and Ozdemir, H. (2009). "Effects of heat treatment on Calabrian pine (Ten.) wood," *BioResources* 4(3), 1032-1043. DOI: 10.15376/biores.4.3.1032-1043

Beran, R., Zarybnicka, L., and Machova, D. (2020). "Recycling of rigid polyurethane foam: Micro-milled powder used as active filler in polyurethane adhesives," *J. Appl. Polym. Sci.* 137(37), article 49095. DOI: 10.1002/app.49095

Chen, Q. S., Ji, Z. J., Chen, J. H., and Wang, J. (2011). "Analysis on the approaches of improving sound insulation performance of lightweight wall," *New Building Materials* 38(05), 31-34. (in Chinese). DOI: 10.3969/j.issn.1001-702X.2011.05.009

de Mello, D., Pezzin, S. H., and Amico, S. C. (2009). "The effect of post-consumer PET particles on the performance of flexible polyurethane foams," *Polymer Testing* 28(7), 702-708. DOI: 10.1016/j.polymertesting.2009.05.014

Demharter, A. (1998). "Polyurethane rigid foam, a proven thermal insulating material for applications between +130°C and −196°C," *Cryogenics* 38(1), 113-117. DOI: 10.1016/S0011-2275(97)00120-3

Demirel, S., and Ergun Tuna, B. (2019). "Evaluation of the cyclic fatigue performance of polyurethane foam in different density and category," *Polymer Testing* 76, 146-153. DOI: 10.1016/j.polymertesting.2019.03.019

Du, H., Zhao, Y. H., Li, Q. F., Wang, J. W., Kang, M. Q., Wang, X. K., and Xiang, H. W. (2008). "Synthesis and characterization of waterborne polyurethane adhesive from MDI and HDI," *J. Appl. Polym. Sci.* 110(3), 1396-1402. DOI: 10.1002/app.28805

Gonultas, O., and Candan, Z. (2018). "Chemical characterization and ftir spectroscopy of thermally compressed eucalyptus wood panels," *Maderas. Ciencia y Tecnología* 20(3), 431-442. DOI: 10.4067/S0718-221X2018005031301

Heiran, R., Ghaderian, A., Reghunadhan, A., Sedaghati, F., Thomas, S., and Haghighi, A. h. (2021). "Glycolysis: An efficient route for recycling of end of life polyurethane foams," *Journal of Polymer Research* 28(1), article 22. DOI: 10.1007/s10965-020-02383-z

Ionescu, M. (2005). *Chemistry and Technology of Polyols for Polyurethanes*. Rapra Technology, Shawbury, Shrewsbury, Shropshire, U.K.

ISO 12999-2:2020 (2020). "Acoustics —Determination and application of measurement uncertainties in building acoustics—Part 2: Sound absorption," International Organization for Standardization, Geneva, Switzerland.

Kemona, A., and Piotrowska, M. (2020). "Polyurethane recycling and disposal: Methods and prospects," *Polymers* (Basel) 12(8). DOI: 10.3390/polym12081752

Krasny, J., Parker, W. J., and Babrauskas, V. (2001). *Fire Behavior of Upholstered Furniture and Mattresses*. Noyes Publications, William Andrew Pub., Park Ridge, N.J., Norwich, N.Y.

Li, J.M., Huang,R., Lv, X. W., Yuan, Y. C., and Xiao, H. (2008). "Application progress of FT-IR technique in polyurethane industry," *Chemical Propellants & Polymeric Materials* 6(6), 30-35+38. (in Chinese). DOI: 10.3969/j.issn.1672-2191.2008.06.008

Mordor Intelligence (2020). "Polyurethane market size & share analysis - Growth trends & forecasts (2023 - 2028)," (https://www.mordorintelligence.com/industry-reports/polyurethane-market).

White, W. R., and Durocher, D. T. (2016). "Recycling of rigid polyurethane articles and reformulation into a variety of polyurethane applications. *Journal of Cellular Plastics* 33(5), 477-486. DOI: 10.1177/0021955X9703300504

Yang, C., Zhuang, Z.-H., and Yang, Z.-G. (2014). "Pulverized polyurethane foam

particles reinforced rigid polyurethane foam and phenolic foam," *J. Appl. Polym. Sci.* 131(1), article 39734. DOI: 10.1002/app.39734

Yang, W., Dong, Q., Liu, S., Xie, H., Liu, L., and Li, J. (2012). "Recycling and disposal methods for polyurethane foam wastes," *Procedia Environmental Sciences* 16, 167-175. DOI: 10.1016/j.proenv.2012.10.023

Zhang, H., Fang, W.-Z., Li, Y.-M., and Tao, W.-Q. (2017). "Experimental study of the thermal conductivity of polyurethane foams," *Applied Thermal Engineering* 115, 528-538. DOI: 10.1016/j.applthermaleng.2016.12.057

Zhao, J., Wang, X.M., Chang, J.M., Yao, Y., and Cui, Q. (2010). "Sound insulation property of wood–waste tire rubber composite," *Composites Science and Technology* 70(14), 2033-2038. DOI: 10.1016/j.compscitech.2010.03.015

Zia, K. M., Bhatti, H. N., and Ahmad Bhatti, I. (2007). "Methods for polyurethane and polyurethane composites, recycling and recovery: A review," *Reactive and Functional Polymers* 67(8), 675-692. DOI: 10.1016/j.reactfunctpolym.2007.05.004

Zygmunt-Kowalska, B., Zakrzewska, P., Szajding, A., Handke, B., and Kuźnia, M. (2023). "Polyurethane foams reinforced with microspheres - Assessment of the application in construction as a thermal insulation material," *Thermochimica Acta* 726, article 179556. DOI: 10.1016/j.tca.2023.179556

Article submitted: April 30, 2024; Peer review completed: June 8, 2024; Revised version received: June 22, 2024; Accepted: June 23, 2024; Published: July 16, 2024.
DOI: 10.15376/biores.19.3.5916-5934